Hindawi
Journal of Nanomaterials
Volume 2019, Article ID 5180460, 7 pages
https://doi.org/10.1155/2019/5180460

Research Article

Gas-Permeable Microimprint Template Derived from Cellulose Nanofiber Derivatives for Mechanical Properties

Seigo Murayama,[1] **Ikuo Motono**,[2] **Kento Mizui**,[2] **Kenji Kondoh**,[1] **Makoto Hanabata**,[2] **and Satoshi Takei**[2]

[1]*Toyama Industrial Technology Research and Development Center, Takaoka, Toyama 933-0981, Japan*
[2]*Prefectural University, Imizu, Toyama 939-0398, Japan*

Correspondence should be addressed to Seigo Murayama; murayama@itc.pref.toyama.jp

Received 28 August 2018; Revised 29 October 2018; Accepted 7 November 2018; Published 18 March 2019

Academic Editor: Ilaria Armentano

A gas-permeable template has lower mechanical properties compared to non-gas-permeable metal templates. Therefore, it is difficult to mass-produce by increasing the area of the gas-permeable template. In this study, we have developed a new gas-permeable template with cellulose nanofiber (CNF) derivatives added to improve the mechanical properties of gas-permeable templates. The reinforcing effect by the CNF derivative added was investigated by a tensile test. As a result, it was shown that Young's modulus was increased about 2 to 3 times by the addition of 2-5 wt% CNF derivative. Also, it was confirmed by confocal microscopic images that transferability and gas permeability of the gas-permeable template were not lost even when the CNF derivative was added.

1. Introduction

A gas-permeable template shown in Figure 1 has attracted attention as a method to reduce pattern defects caused by air trapping and outgas generated by solvents between a template and an imprinting material [1–7]. The gas-permeable template increases the area required for mass production owing to lower mechanical properties as compared with those of a non-gas-permeable metallic template.

Compositing a resin with glass fiber or carbon fiber is a well-known method of increasing the mechanical properties of a material [8–12]. Particularly, cellulose nanofibers (CNF) formed via the high-pressure wet jet mill method are characterized by their high strength and low thermal expansion, and unlike glass fibers, they do not turn opaque when compounding into materials or require complex treatment because of a plant-derived material during disposal [13–17]. Therefore, CNF is considered as an alternative material for automobile and aircraft parts [18].

In this study, we focused on the reinforcing effect of CNF and attempted to develop a new template model for improving the mechanical properties by adding CNF to the conventional gas-permeable template material. In addition, we investigated their mechanical properties by the tensile test. Further, in order to check whether gas permeability and precision transferability of the gas permeable template are not lost by addition of CNF, an acrylic ultraviolet (UV) cross-linked liquid material containing methyl ethyl ketone (MEK) was patterned and observed with a microscope.

2. Materials and Methods

2.1. Preparation of the Thermoset Cellulose Derivative for a Gas-Permeable Microimprint Template. As a matrix of gas-permeable microimprint template, a thermal cross-linkable cellulose derivative with acrylate groups (HPC-AOI) was synthesized using 2-acryloyloxyethyl isocyanate (Showa Denko) and hydroxypropyl cellulose (Wako Pure Chemical Industries). The chemical structures and reactions of

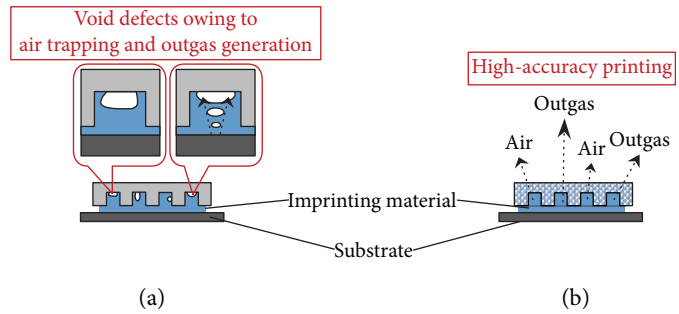

Figure 1: UV-imprint process using (a) a conventional template that causes void defects owing to air trapping and outgas generation and (b) a gas-permeable template that results in high-accuracy printing.

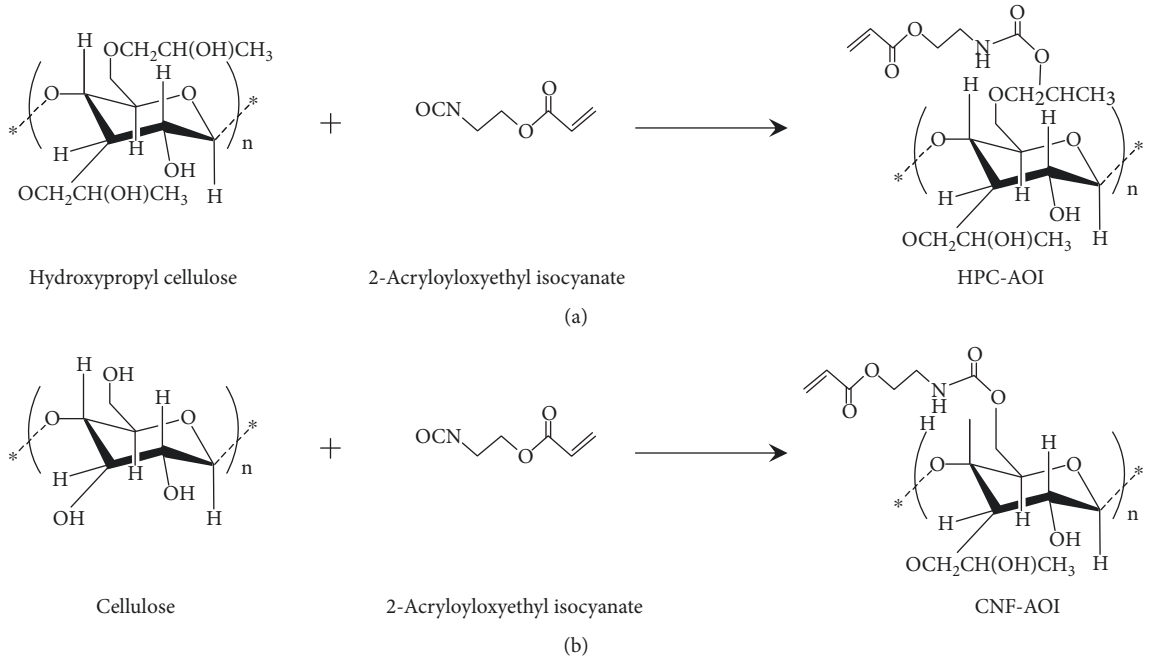

Figure 2: (a) Chemical reaction between hydroxypropyl cellulose (HPC) and 2-acryloyloxyethyl isocyanate and structure of gas-permeable template matrix (HPC-AOI). (b) Chemical reaction between cellulose nanofiber (CNF) and 2-acryloyloxyethyl isocyanate and structure of gas-permeable template reinforcement (CNF-AOI).

hydroxypropyl cellulose, 2-acryloyloxyethyl isocyanate, and HPC-AOI are shown in Figure 2(a). Hydroxypropyl cellulose was combined with 2-acryloyloxyethyl isocyanate and MEK for 3 h in a 1,1,1,2-tetrafluoroethane-rich atmosphere. 2-acryloyloxyethyl isocyanate was added in an amount corresponding to 20% of the hydroxyl groups of hydroxypropyl cellulose. Then, triethylamine (Kanto Chemical Co. Ltd.) was added to a concentration of 8.9 wt% based on the total weight, and the mixture was stirred at 60°C for 80 min in a 1,1,1,2-tetrafluoroethane-rich environment.

2.2. Preparation of CNF for a Gas-Permeable Microimprint Template. A thermal cross-linkable CNF derivative with acrylate groups (CNF-AOI) was synthesized using 2-acryloyloxyethyl isocyanate and CNF to be used as a filler in the gas-permeable biomass template. CNF was prepared by dispersing a suspension of 2 wt% concentration of cellulose crystal (Asahi Kasei) and MEK (Taiyou Chemical) with a high-pressure wet jet mill (HJP-25005, Sugino Machine Limited) at 200 MPa. The chemical structures and reactions of CNF, 2-acryloyloxyethyl isocyanate, and CNF-AOI are shown in Figure 2(b). CNF dispersed in MEK was mixed with 2-acryloyloxyethyl isocyanate under a 1,1,1,2-tetrafluoroethane-rich atmosphere for 3 h. Triethylamine (Kanto Chemical Co. Ltd.) was added to a concentration of 8.9 wt% based on the total weight and was stirred at 50°C in a 1,1,1,2-tetrafluoroethane-rich atmosphere. Since CNF has lower solubility than HPC, the stirring time in CNF-AOI synthesis was set to 7 hours.

2.3. Analysis of CNF and Synthetic Materials. The conversion of cellulose to nanofibers using the high-pressure jet mill was

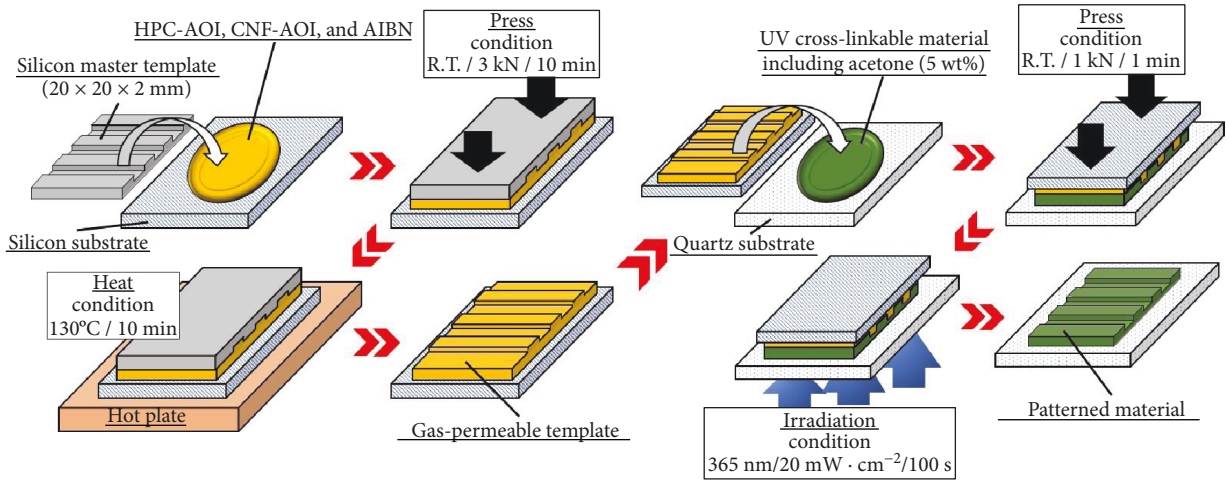

Figure 3: Flow chart of template preparation and imprint process with a UV-cross-linkable material with acetone, using HPC-MOI and HPC-AOI templates.

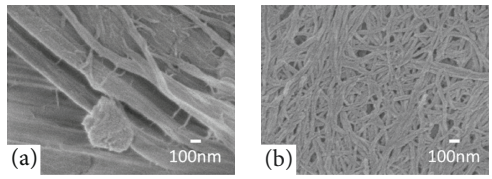

(a) (b)

Figure 4: FE-SEM images: (a) cellulose before dispersion and (b) CNF after dispersion process.

observed via field emission scanning electron microscopy (FE-SEM). The observation magnification of FE-SEM was set to 50,000 times.

The Fourier-transform infrared spectroscopy measurement using the attenuated total reflection method (ATR-FTIR) was performed to confirm the synthesis results of HPC-AOI and CNF-AOI.

2.4. Mechanical Properties of the HPC-AOI and CNF-AOI. 2,2′-Azodiisobutyronitrile having concentration (AIBN; Tokyo Kasei) was prepared as a thermal radical polymerization initiator, added to the HPC-AOI in MEK, and stirred for 2 min in a blender. Furthermore, CNF-AOI was added to the solution and stirred for 2 min. The mixture was dropped onto a mold, and films were formed using a vacuum oven (AVO-310N, AS ONE). Baking conditions included a temperature of 20°C for 2 h under a diminished pressure of 0.04 MPa. Following this, a tensile test sample piece was punched out of the film using a punching machine. Three points were measured: thickness (h), length (L), and width (b_1) using a micrometer, and the cross sectional area (A) was calculated based on the average value. The sample was measured using a tensile tester (EZ-LX, Shimadzu), and the stress (σ) was determined from the loads (P) using equation (1). The strain (ε) was determined from the stroke (ΔL) (equation (2)).

In the tensile test, the reinforcing effect of CNF was confirmed by comparing Young's modulus with the sample to which CNF-AOI was added, using the sample to which CNF-AOI was not added as a reference.

$$\sigma(\text{MPa}) = \frac{P\,(N)}{A\,(\text{mm}^2)} = \frac{P\,(N)}{b_1\,(\text{mm}) \times h\,(\text{mm})}, \quad (1)$$

$$\varepsilon(\%) = \frac{\Delta L\,(\text{mm})}{L_0\,(\text{mm})}. \quad (2)$$

2.5. Film Preparation and Analysis. HPC-AOI and CNF-AOI templates were imprinted from a quartz master substrate that featured a 2 μm line and space and a 3 μm height. Ultraviolet and thermal cross-linking imprint lithography was conducted by employing an imprint test machine (Litho Tech Japan STIE-400). The procedure was employed as follows (Figure 3) [19]: (1) a mixture of AIBN, HPC-AOI, and CNF-AOI was cast onto a silicon substrate (20 × 20 × 2.4 mm); (2) the HPC-AOI and CNF-AOI were kept in contact with the quartz master template for 10 min at room temperature and imprinted at 7 kgf; (3) the thermal polymerization reaction for these materials was conducted at 130°C for 10 min; (4) the HPC-AOI and CNF-AOI gas-permeable templates were obtained after demolding from the master template; (5) the acrylic UV-curable liquid material with 5 wt% acetone was placed on the quartz substrate that was spin coated with an underlayer; (6) after leaving the substrate at room temperature for 90 s, the material was pressed into the HPC-AOI and CNF-AOI templates at room temperature at 1 kN for 1 min.

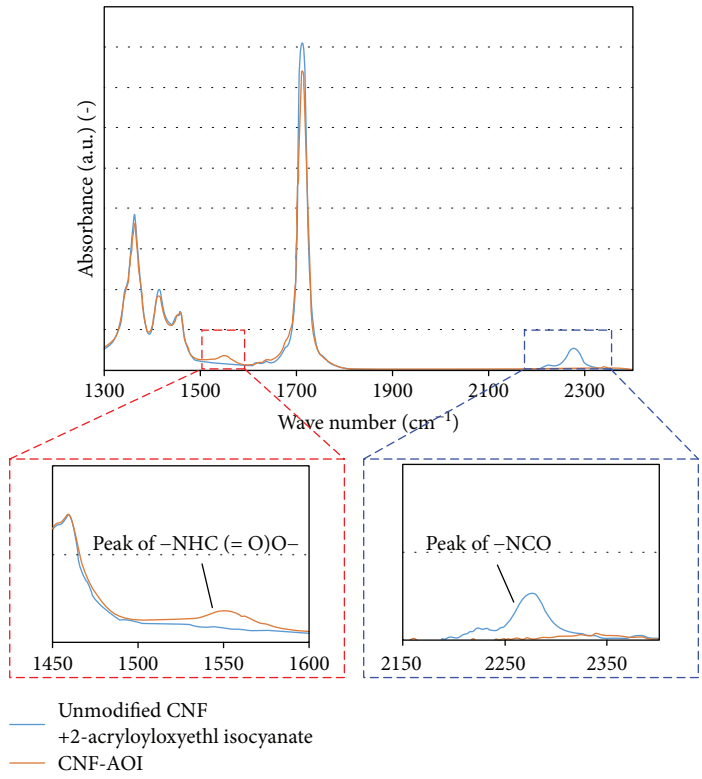

Figure 5: FT-IR spectrum of CNF-AOI.

The fixing chemical reaction of the UV-curable material was performed under UV irradiation with a peak value of 365 nm and an intensity of 20 mW/cm^2 for 60 s using a high-pressure mercury vapor lamp (Hoya Candeo Optronics EX250); and (7) after removing the template from the imprinted UV-curable material, the structure was observed using a confocal microscope (Lasertec OPTELICS H1200). The gas permeability and precision transfer of the HPC-AOI and CNF-AOI templates were investigated through this microscope image.

3. Results and Discussion

3.1. Analysis of CNF and Synthetic Materials. Figures 4(a) and 4(b) show the FE-SEM images of cellulose before the dispersion process and CNF after the dispersion process, respectively. Based on these images, it was confirmed that cellulose with a fiber diameter ≥ 100 nm turned into a nanofiber with a 20 nm fiber diameter using the high-pressure wet jet mill.

The synthesis of CNF derivatives can be confirmed by capturing changes in the characteristic chemical bond spectral regions of hydroxypropyl cellulose and 2-acryloyloxyethyl isocyanate by FT-IR measurement. The first is an -NCO stretching vibration at 2275-2250 cm^{-1} and the second is -HNCO stretching and bending vibration at 1550–1510 cm^{-1} [20]. Figure 5 shows the FT-IR spectra of the CNF-AOI solution, i.e., unmodified CNF and 2-acryloyloxyethyl isocyanate in MEK. In the CNF-AOI spectrum, the absorption of HNCO increased as the absorption of -NCO decreased. Conversely, in the 2-acryloyloxyethyl isocyanate spectrum, the absorption of HNCO decreased as the absorption of -NCO increased. Thus, the synthesis of CNF-AOI was confirmed.

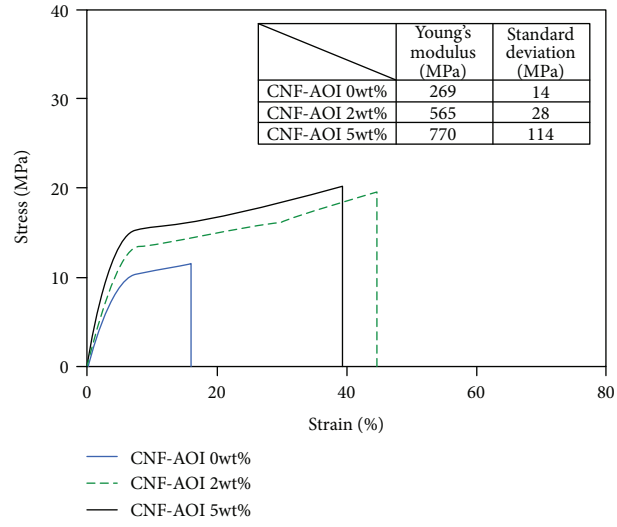

Figure 6: Stress-strain curve and mechanical properties when changing CNF-AOI concentration to values 0, 2, and 5 wt% for HPC-AOI.

3.2. Mechanical Properties of the HPC-AOI and CNF-AOI. In the tensile test, the reinforcing effect of CNF-AOI on HPC-AOI was investigated by varying the CNF-AOI concentration to the values 0, 2, and 5 wt%. Figure 6 shows the stress-strain curve and mechanical properties obtained from the test. Young's modulus (E) was obtained from the slope of

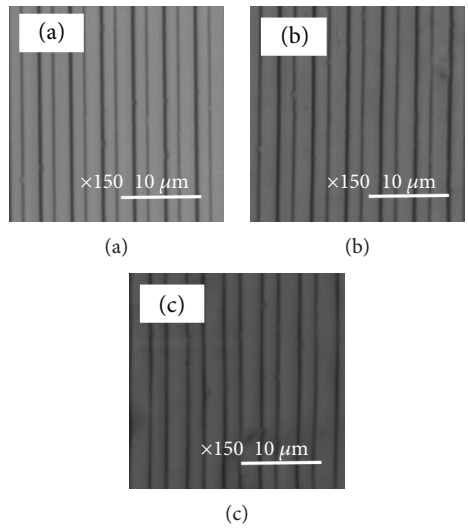

Figure 7: Confocal microscopic images of the 2 μm line and space pattern templates: (a) HPC-AOI template, (b) HPC-AOI template with CNF-AOI 2 wt%, and (c) HPC-AOI template with CNF-AOI 5 wt%.

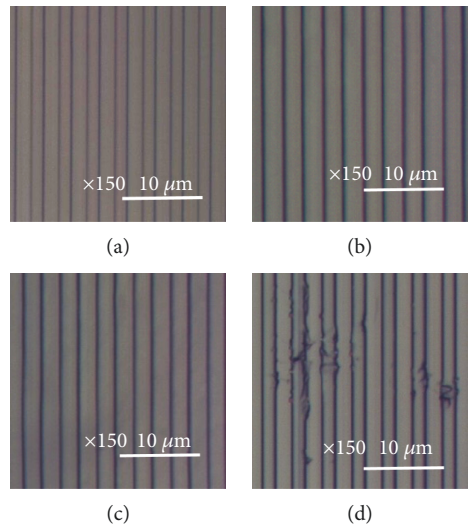

Figure 8: Confocal microscopic images of the UV-cross-linked liquid material containing acetone imprinted using (a) HPC-AOI template, (b) HPC-AOI template with CNF-AOI 2 wt%, (c) HPC-AOI template with CNF-AOI 5 wt%, and (d) conventional silicon template.

the stress-strain curve using equation (3), when the force used in the test ranged from 3 to 5 N. Young's modulus of the samples containing CNF 2-5 wt% was predicted to be 2.1–2.9 times larger than that of CNF 0 wt%. In terms of Young's modulus, CNF 0 wt% corresponded to low-density polyethylene and CNF 5 wt% corresponded to high-density polyethylene. In addition, the values of other mechanical properties also increased, when CNF-AOI was added. CNF 0 wt% was brittle due to the small tensile strength and breaking stress; however, CNF 2–5 wt% exhibited high toughness as the tensile strength and breaking stress increased. The tensile strength was at the maximum at CNF 5 wt%, and the rupture stress was at the maximum at 2 wt%. However, the difference was small. Therefore, it was suggested that these properties do not depend on the amount of the added CNF.

In terms of the standard deviation, the CNF-AOI 0 or 2 wt% sample had small fluctuations in Young's modulus. These tensile samples were prepared by stamping out the film in a random direction, so it suggested that there is no anisotropy of tensile strength in the longitudinal direction and the transverse direction. Also, it suggested that 2 wt% of CNF-AOI was uniformly dispersed in HPC-AOI. On the other hand, the 5 wt% sample of CNF-AOI showed a large fluctuation in Young's modulus. There seemed to be two reasons for it. First, the addition of CNF-AOI increases the viscosity of the solution before film formation, resulting in insufficient dispersion. The second was that the number of CNF-AOI present in HPC-AOI increased, making it difficult for CNF-AOI to uniformly arrange in HPC-AOI. Therefore, when increasing the additional amount of CNF-AOI, the CNF-AOI dispersion process becomes very important.

In any case, these results suggest that the mechanical properties of a gas-permeable microimprint template are improved by the addition of CNF-AOI.

$$E\,(\mathrm{MPa}) = \frac{\sigma\,(\mathrm{MPa})}{\varepsilon\,(\%)}. \quad (3)$$

Jonoobi and coworkers reported similar improvements for polylactic acid (PLA) nanocomposites with CNF 5 wt% CNF content [21].

3.3. Gas-Permeable Microimprint Template Analysis. Figures 7(a)–7(c) show the confocal microscopic images of the 2 μm line and space pattern templates that were HPC-AOI template, HPC-AOI template with CNF-AOI 2 wt%, and an HPC-AOI template with CNF-AOI 5 wt%, respectively. As irregularities and defects were not found in all the images, it was confirmed that the structure of the master template was accurately transferred to all templates. This result suggests that the addition of CNF-AOI does not affect transferability and that the template can be prepared via a conventional method.

Figures 8(a)–8(d) show the confocal microscopic images of the UV-cross-linked liquid material containing an acetone template imprinted using HPC-AOI template, HPC-AOI template with CNF-AOI 2 wt%, HPC-AOI template with CNF-AOI 5 wt%, and silicon template, respectively. In the pattern using a silicon template that is not gas-permeable, defects were observed that were deemed to be generated by the volatilization of acetone. On the other hand, the pattern obtained using the HPC-AOI template displayed gas permeability as such defects were not observed. Similarly, the absence of defects in Figures 8(b) and 8(c) suggested that gas permeability was not lost even when CNF-AOI was added.

4. Conclusion

The thermoset cellulose derivative, CNF-AOI, was obtained by reacting 2-acryloyloxyethyl isocyanate and CNF formed using a high-pressure wet jet mill, to be used as a material for increasing the template's mechanical properties. The FT-IR spectrum of the reagents showed the formation of CNF-AOI. Young's modulus was observed to increase about 2–3 times due to the addition of CNF-AOI when the mechanical properties of the HPC-AOI template were compared to those of the HPC-AOI-added 2-5 wt% CNF-AOI template. We considered that the HPC-AOI-added 2-5 wt% CNF-AOI template had precision transferability because these confocal microscopic images showed no pattern defects and void defects.

Finally, it was suggested that the HPC-AOI-added CNF-AOI template was able to increase the area required for mass production because it yielded increased mechanical properties.

Data Availability

The gas-permeable template data and Young's modulus data used to support the findings of this study were cited at relevant places within the text as references [1–7, 20].

Conflicts of Interest

The authors declare that there is no conflict of interest regarding the publication of this paper.

Acknowledgments

This project was supported by Toyama Nanotech Cluster of the Ministry of Education, Culture, Sports, Science and Technology, Japan; JSPS KAKENHI No. 16K04920; JST Program No. VP29117936791; JSPS Bilateral Joint Research Projects 2017 in Belgium; the Ogasawara Foundation; the Amada Foundation; the Canon Foundation; the Die and Mould Technology Promotion Foundation; the Osawa Scientific Studies Grants Foundation; Advanced Machining Technology and Development Association; and the Mazak Foundation.

References

[1] S. Takei and M. Hanabata, "Ultraviolet nanoimprint lithography using cyclodextrin-based porous template for pattern failure reduction," *Applied Physics Letters*, vol. 107, no. 14, article 141904, 2015.

[2] S. Takei and M. Hanabata, "Sub-70 nm resolution patterning of high etch-resistant epoxy novolac resins using gas permeable templates in ultraviolet nanoimprint lithography," *Applied Physics Express*, vol. 9, no. 5, article 056501, 2016.

[3] S. Takei, S. Nakajima, K. Sugahara, M. Hanabata, Y. Matsumoto, and A. Sekiguchi, "Gas-permeable cellulose template for reduction of template damage and gas trapping in microimprint lithography of high volume manufacturing," *Macromolecular Materials and Engineering*, vol. 301, no. 8, pp. 902–906, 2016.

[4] M. Hanabata, S. Takei, K. Sugahara et al., "Nanoimprint lithography using disposable biomass template," in *Proceedings of SPIE 9777, Alternative Lithographic Technologies VIII*, vol. 97771G, San Jose, CA, USA, April 2016.

[5] S. Nakajima, S. Takei, Z. Zhou et al., "Development of nanoimprint lithography template materials using biomass," *Journal of Photopolymer Science and Technology*, vol. 29, no. 2, pp. 189–193, 2016.

[6] N. Sugino, S. Takei, S. Nakajima, M. Hanabata, T. Kameda, and A. Sekiguchi, "Characterization of gas permeable template material for nanoimprinting," *Journal of Photopolymer Science and Technology*, vol. 30, no. 3, pp. 275–280, 2017.

[7] S. Nakajima, S. Takei, M. Hanabata et al., "High resolution patterning of ultraviolet cross-linked resins using gas permeable mold derived from cellulose in nanoimprint lithography," in *Proceedings of SPIE 10354, Nanoengineering: Fabrication, Properties, Optics, and Devices XIV*, vol. 103541B, San Diego, CA, USA, August 2017.

[8] M. Miki, T. Fukuda, and S. Motoki, *Fukugouzairyou (Composite Material)*, Kyoritsu Shuppan Co., Ltd., 1997.

[9] F. Ide, *Tokuseibetuniwakarujituyoukoubunshizairyou (Practical Polymer Materials Understood by Characteristics)*, Kogyo Chosakai Publishing Co., Ltd., 2002.

[10] Y. Miyano, M. Kanemitsu, T. Kunio, and H. Kuhn, "Role of matrix resin on fracture strengths of unidirectional CFRP," *Journal of Composite Materials*, vol. 20, no. 6, pp. 520–538, 1986.

[11] Y. Miyano, M. Nakada, and H. Cai, "Formulation of long-term creep and fatigue strengths of polymer composites based on accelerated testing methodology," *Journal of Composite Materials*, vol. 42, no. 18, pp. 1897–1919, 2008.

[12] T. Ohsawa, A. Nakayama, M. Miwa, and A. Hasegawa, "Temperature dependence of critical fiber length for glass fiber-reinforced thermosetting resins," *Journal of Applied Polymer Science*, vol. 22, no. 11, pp. 3202–3212, 1978.

[13] A. Isogai, M. Kawasaki, and H. Yano, *Technical Data of Cellulose Nanofibers*, CMC publishing, 2016.

[14] H. Matumura, K. Ogura, K. Kondoh et al., *Cellose Nanofiber*, Johokiko Co., Ltd, 2018.

[15] Y. Watanabe, S. Kitamura, K. Kawasaki et al., *Biopolymers*, vol. 95, no. 12, pp. 833–839, 2011.

[16] K. Ogura, "Baiomasunanofuaiba' BiNFi-s' nituite," *Kougyouzairyou (Industrial materials)*, vol. 63, no. 10, pp. 73–76, 2015.

[17] K. Ogura, "CNFtokikinzokunanoryushinofukugokashuho," *Kagakusouchi (Chemical equipment)*, vol. 59, no. 9, pp. 21–23, 2017.

[18] J. Dlouhá, L. Suryanegara, and H. Yano, "Cellulose nanofibre–poly(lactic acid) microcellular foams exhibiting high tensile toughness," *Reactive and Functional Polymers*, vol. 85, pp. 201–207, 2014.

[19] S. Nakajima, S. Takei, S. Takamatsu et al., "Gas-permeable templates using cellulose derivatives with acrylate and methacrylate groups for reducing in void defect density in ultraviolet nanoimprint lithography," *Japanese Journal of Applied Physics*, vol. 57, no. 8, p. 086503, 2018.

[20] M. Hesse, H. Meier, and B. Zeeh, *Spectroscopic Methods in Organic Chemistry*, Kagaku-Dojin Publishing Company, Inc., 2010.

[21] M. Jonoobi, J. Harun, A. P. Mathew, and K. Oksman, "Mechanical properties of cellulose nanofiber (CNF) reinforced polylactic acid (PLA) prepared by twin screw extrusion," *Composites Science and Technology*, vol. 70, no. 12, pp. 1742–1747, 2010.